

# Scanning of nickel sulfamate concentration in electrodeposition bath used for production of Ni–Co alloys

Ali Karpuz · Hakan Kockar · Mursel Alper

Received: 7 February 2013 / Accepted: 23 April 2013 / Published online: 3 May 2013  
© Springer Science+Business Media New York 2013

**Abstract** The Ni–Co films were produced by using the electrodeposition technique from the electrolytes with different  $\text{Ni}(\text{SO}_3 \cdot \text{NH}_2)_2 \cdot 4\text{H}_2\text{O}$  concentrations (from 0 to 0.45 M). The Ni content of the films changed gradually from 0 to 57 %. The Ni–Co system exhibited anomalous codeposition. For 0 at.% Ni content, the saturation magnetization,  $M_s$  of the film was found to be  $1298 \text{ emu/cm}^3$ , which is close to that of bulk Co ( $1420 \text{ emu/cm}^3$ ). As the Ni content increased,  $M_s$  decreased since the  $M_s$  value of bulk Ni ( $480 \text{ emu/cm}^3$ ) is lower than that of bulk Co. The coercivity,  $H_c$ , of Co film was found as 37 Oe. When the Ni content increased to 6 at.%, the  $H_c$  value dramatically increased to 109 Oe. The hexagonal closed packed (hcp) structure was observed for the films containing 0 and 6 at.% Ni. When the Ni content increased to 25 at.%, a mixed phase of face centered cubic (fcc) and hcp structure (mostly fcc) was detected. For further increase in Ni content (39 and 57 at.%), the peaks which occurred from the reflections of fcc phase were obtained. As a result of structural analysis, the Co content can be determined as 62–64 at.% for changing of crystal structure. The transfiguration from spherical granular to acicular surface morphology occurred around 75 at.% Co content.

Magneto-resistance of the films was measured and it was found that the films show anisotropic magneto-resistance.

## 1 Introduction

Electrochemical production of magnetic layers is very useful method due to controllable experimental conditions [1]. Furthermore, it has considerable advantages like rapid production, low cost and easy control in terms of deposition parameters [2]. Many kinds of magnetic films can be produced with electrodeposition [3, 4]. Among these films, Ni–Co alloys are utilized in important applications because of their unique properties such as magnetic, heat conductivity and strength [5]. Magnetic properties of these alloys also provide a large usage and many advantages in engineering applications [6]. Also, Ni–Co films are important materials for investigation of magnetic properties and have been widely studied by scientist. Because the magnetic properties of Ni–Co films are significantly affected by their microstructural properties as well as their film content [7], the systematic characterizations of compositional and structural properties are primary topics for investigations. There are several studies reported the changes in properties of Ni–Co alloys caused by different experimental conditions. Whereas the studies [8] and [9] have concentrated on the effect of the current density and temperature on properties of Ni–Co films, respectively, the studies [1] and [10] investigated the influence of pH and the behavior of corrosion resistance, respectively. Also, the earlier studies [5, 9, 11] have indicated that the Ni content has a significant effect on the properties of electrodeposited Ni–Co films.

The aim of this study is to investigate the properties of Ni–Co films, which were deposited by changing the Ni concentration of the electrolyte. The crystal structure and the

A. Karpuz (✉)  
Physics Department, Kamil Ozdag Science Faculty,  
Karamanoglu Mehmetbey University, Yunus Emre Yerleşkesi,  
70100 Karaman, Turkey  
e-mail: alikarpuz@kmu.edu.tr

H. Kockar  
Physics Department, Science and Literature Faculty,  
Balıkesir University, Balıkesir, Turkey

M. Alper  
Physics Department, Science and Literature Faculty,  
Uludağ University, Bursa, Turkey

surface morphology of the films change with the Ni concentration, and hence depending on the Ni content of the films as well as magnetic and magnetoresistance (MR) properties.

## 2 Experimental

Ni–Co films were electrodeposited at room temperature from the unstirred electrolytes with different nickel sulfamate concentrations. The baths with following concentrations were used for electrochemical deposition: 0–0.45 M  $\text{Ni}(\text{SO}_3 \cdot \text{NH}_2)_2 \cdot 4\text{H}_2\text{O}$ ; 0.2 M  $\text{CoSO}_4 \cdot 7\text{H}_2\text{O}$ ; 0.2 M  $\text{H}_3\text{BO}_3$ . All electrolytes were prepared by using distilled water. A potentiostat/galvanostat (EGG Model 362) with three electrodes was used for depositions. A titanium plate was used as substrate and a platinum plate was used as counter electrode while the reference electrode was a saturated calomel electrode (SCE). The surface area of the substrate was  $2.88 \text{ cm}^2$  and the same area was used for all depositions. All potentials were adjusted with respect to the SCE. For codeposition of Ni and Co ions, the cathode potential was determined by considering the cyclic voltammetry analysis which was done in our earlier study [7]. Hence, the all depositions were carried out at  $-1.9 \text{ V}$ . The pH of the electrolytes which were used for deposition was  $2.85 \pm 0.05$  and the thickness of the films was chosen as  $3 \mu\text{m}$ . The choice of this pH, thickness and electrolyte concentration value was based on some preliminary production to get appropriate film structure for characterization. After deposition, the Ni–Co films were peeled off from their substrates and preserved under proper conditions.

The compositional analysis was achieved by using an energy dispersive x-ray spectroscopy (EDX, GENESIS APEX 4—EDAX, AMETEK). The magnetic investigation was done by a vibrating sample magnetometer (VSM, ADE TECHNOLOGIES DMS-EV9). X-ray diffraction (XRD) results were obtained by using an x-ray diffractometer (PANalytical) with  $\text{Cu-K}\alpha$  radiation by scanning  $2\theta$  between  $40^\circ$  and  $100^\circ$ . The surface morphology of the films was observed by a FEI<sup>TM</sup>, NOVA NANOSEM 430 scanning electron microscope (SEM). MR measurements were carried out by using the van der Pauw geometry with four point probes [12]. The applied magnetic field was in the film plane and it was changed between  $\pm 10 \text{ kOe}$ . The electric current was applied both parallel and perpendicular to the magnetic field for measurements of longitudinal (LMR) and transverse magnetoresistance (TMR), respectively, as in [13]. To calculate the percentage changes in MR, the equation given in Ref. [14] was used.

## 3 Results and discussion

A series of Ni–Co films was produced from the electrolytes containing different Ni concentrations. In other words,

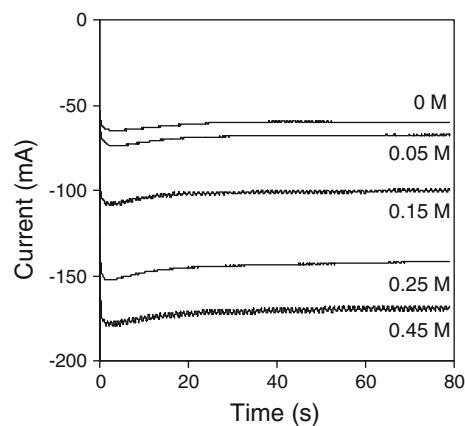


**Fig. 1** Current–time transients of the films

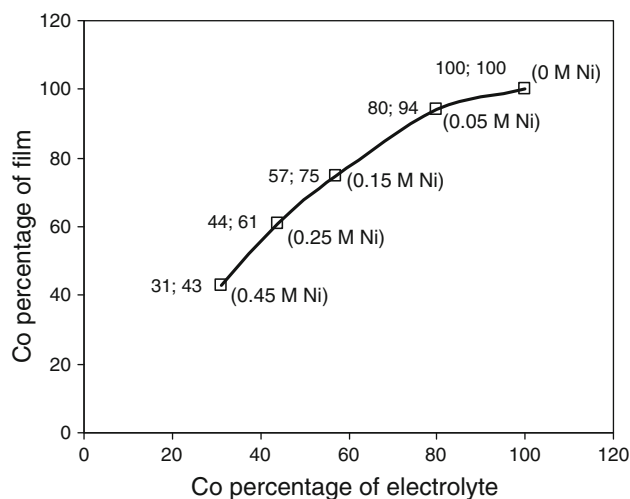


**Fig. 2** Co contents of the films as a function of Co ion concentrations of the electrolytes

while the  $\text{CoSO}_4$  and  $\text{H}_3\text{BO}_3$  concentrations were kept at the constant values (0.2 M), the  $\text{Ni}(\text{SO}_3 \cdot \text{NH}_2)_2$  concentration was adjusted as 0, 0.05, 0.15, 0.25, 0.45 M. To control deposition processes, the current–time transients were obtained during the depositions as done in [11]. The transients were given in Fig. 1 for each film. It was understood that the current intensity which occurred between electrodes during deposition increased when the Ni ion concentration was increased. The increase of current intensity can be explained with increase in amount of metal ions that participated to the depositions. Similar behavior was seen in study [15] that reported the role of Cu content on properties of Fe–Cu films. On the other hand, the current also increases in the current–time transient of the study [16], when the cathode potential is increased. Furthermore, the current intensity values remained almost at a stable value for each film (see Fig. 1). This stability implies that the metal ions were uniformly deposited and charge of deposition was almost in a constant value for each deposition separately.

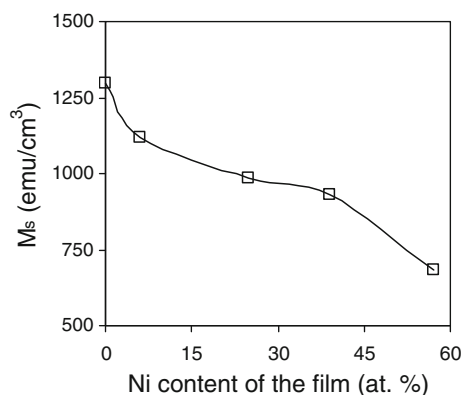


**Fig. 3** Dependence of  $M_s$  on Ni content of the films

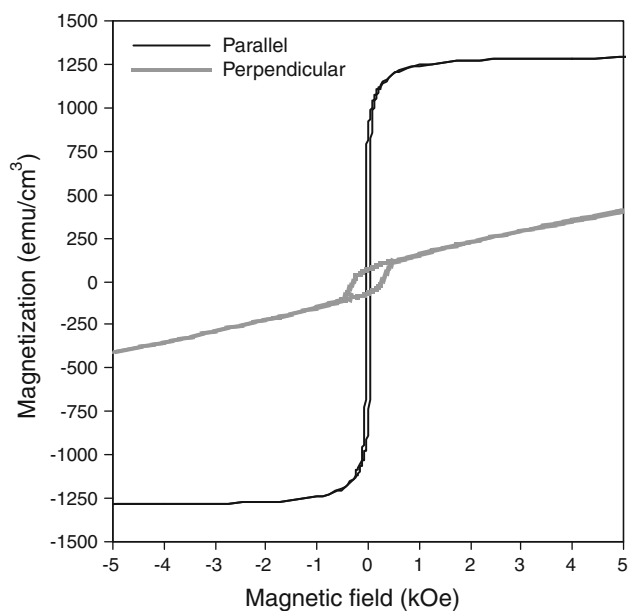


**Fig. 4** In-plane (*parallel*) and perpendicular hysteresis loops of the Co film

According to compositional analysis, when the Ni concentration was changed from 0 to 0.45 M, the Ni content of the films varied gradually in the region of 0–57 at.%. In other words, the Ni content was found as 0, 6, 25, 39 and 57 at.% for the films deposited from the electrolytes containing 0, 0.05, 0.15, 0.25, 0.45 M  $\text{Ni}(\text{SO}_3 \cdot \text{NH}_2)_2$  concentrations, respectively. The rest of the films was detected as Co atoms. It is obvious that increasing Ni concentration leads to increasing Ni content in the film. Similarly, in study [12] which investigated Co–Fe films, Fe content of films increased from around 1 to around 28 % when concentration of Fe was increased from 0.01 to 0.12 M. Figure 2 indicates the percentage of Co in the films according to Co percentage in the electrolyte. It was detected that percentage of Co in the films was higher than Co percentage of the electrolyte for all films deposited. This is described as

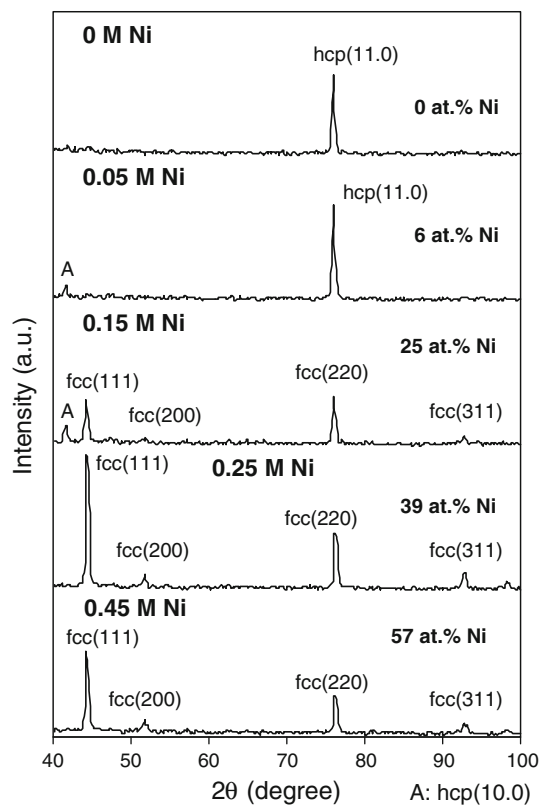


**Fig. 5** XRD patterns of the films deposited with different Ni concentrations

anomalous codeposition as found in [5, 7]. The results also revealed that the anomalous type of Co and Ni codeposition can be seen for Co electrolyte concentration of 57–100 %. This concentration region was unexplained in our earlier studies [7, 11].

In the point of magnetic properties, saturation magnetization,  $M_s$  and coercivity,  $H_c$  were considered and characterized as a function of film content. The  $M_s$  values of the films were found as 1298, 1117, 985, 931, 683  $\text{emu/cm}^3$  for the films with 0, 6, 25, 39 and 57 % at. Ni content, respectively (see Fig. 3). Since the  $M_s$  value of a magnetic film depends mainly on its film content and the  $M_s$  value of bulk Ni is lower than that of bulk Co [17], the  $M_s$  value decreased as the Ni content increased for the Ni–Co films electrodeposited in this study. This is an expected case for Ni–Co alloys. The same change of  $M_s$  can also be seen in study [18] that investigated Ni–Fe films. The acquired values in this study are generally compatible with our earlier study [7] which investigated the Ni–Co films in the region of 0–80 at.% Co content. Furthermore, the study also reported the  $M_s$  and  $H_c$  values for pure Co film (0 M Ni) which was unexplained in [7]. The in-plane (*parallel*) hysteresis loop of the Co film was plotted in Fig. 4. The in-plane  $H_c$  of the Co film was found as 37 Oe. When the Ni content of the film was 6 at.% (0.05 M Ni) the  $H_c$

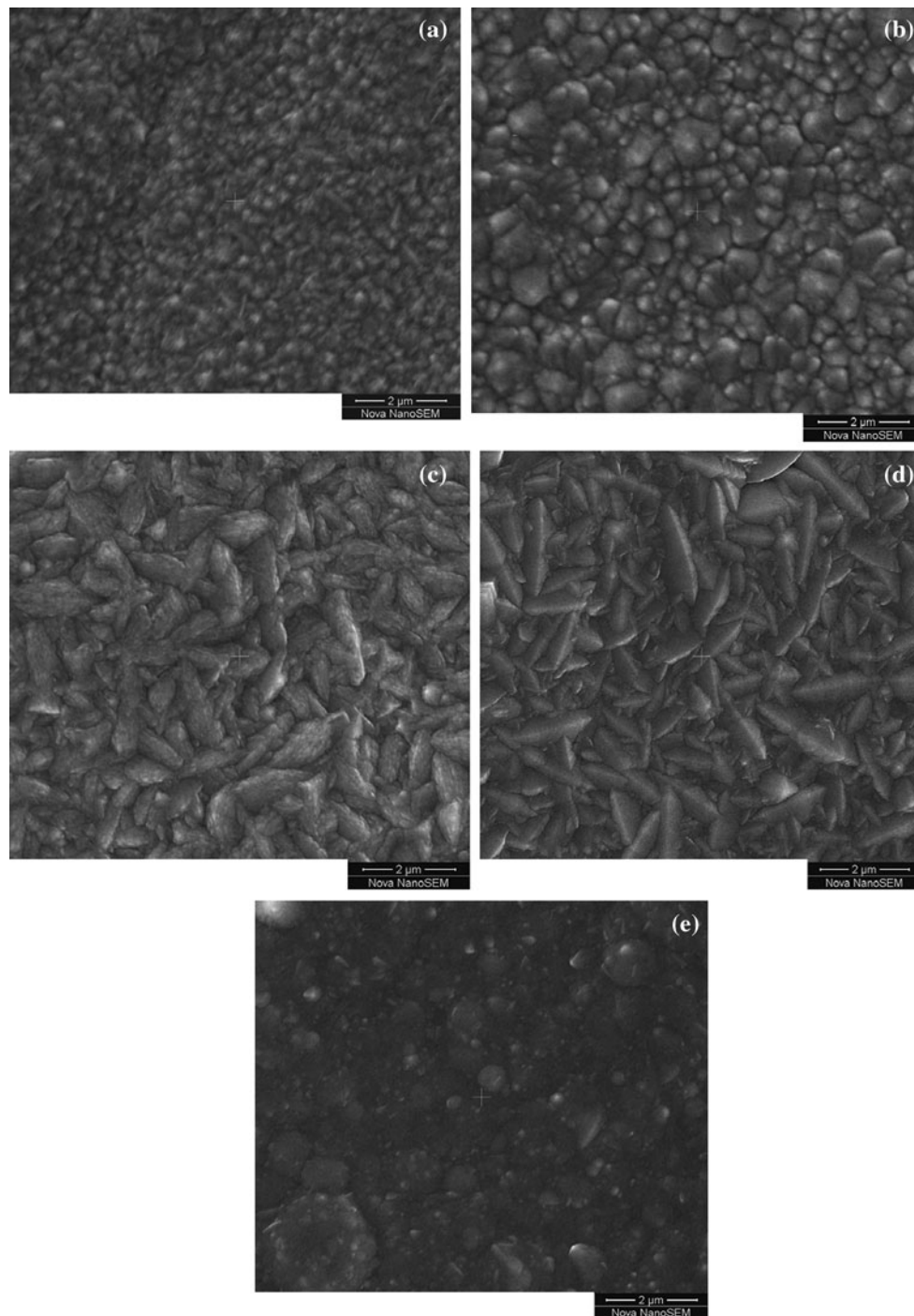


**Fig. 6** SEM micrographs of the films, **a** 0 M (0 at.% Ni), **b** 0.05 M (6 at.% Ni), **c** 0.15 M (25 at.% Ni), **d** 0.25 M (39 at.% Ni), **e** 0.45 M (57 at.% Ni)

dramatically increased to 109 Oe and remained almost at this value (105 Oe) for the film containing 25 at.% Ni content (0.15 M Ni). The reason of these high  $H_c$  values was associated with change in crystal structure of films and discussed in results of XRD analysis. Similarly, a large difference in  $H_c$  values was previously detected in study [19] for Co film and the film with  $\sim 20\%$  Ni content by

using chloride bath. For the higher Ni contents (39 and 57 at. %), the in-plane  $H_c$  values decreased to 43 Oe. It was understood that the in-plane  $H_c$  of the Ni–Co films has the peak values in the region of 6–25 at.% Ni content and it is difficult to magnetize these films compared to the other films which were characterized in this study. The  $H_c$  values confirm the values found in study [7] for the region of

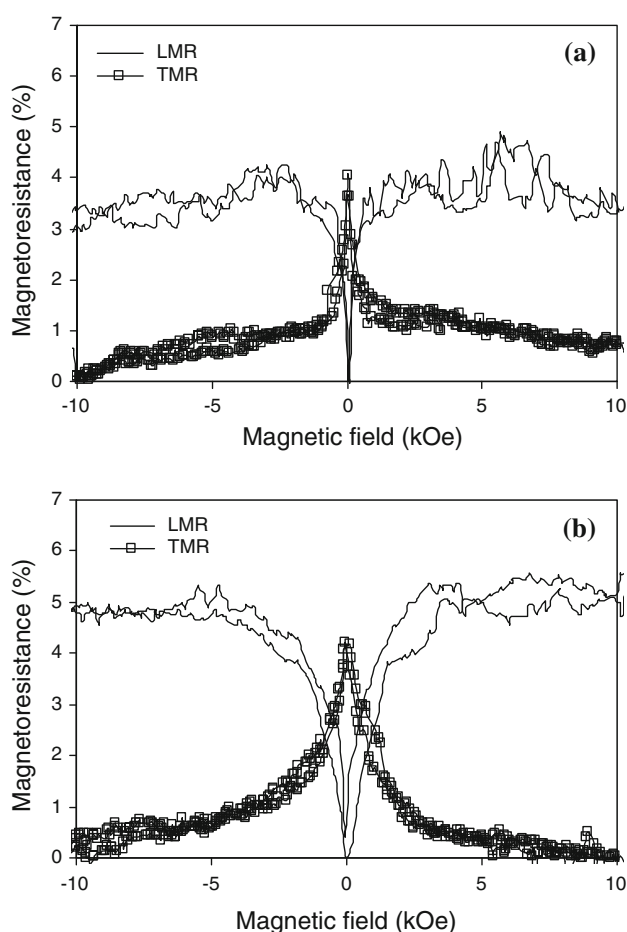


**Fig. 7** LMR and TMR curves of the films, **a** 0 M (0 % Ni film content), **b** 0.05 M (6 % Ni film content)

40–80 at.% Co content. The perpendicular hysteresis loop was also obtained by applying the magnetic field perpendicular to the surface of Co film, see Fig. 4. Since the in-plane hysteresis loop has a higher remanent magnetization and a lower  $H_c$  value than perpendicular loop, it can be understood that the easy-axis direction of the magnetization is in the film plane due to the shape magnetic anisotropy.

The XRD patterns of the films were presented in Fig. 5. As seen in the figure, only one diffraction peak was observed at  $2\theta \sim 76^\circ$  in the XRD pattern of the pure Co film. Because Co has the hexagonal closed packed (hcp) crystal structure [7], this main peak can be supposed as the hcp (11.0) peak. The hcp phase was also obtained for the film produced from 0.05 M nickel sulfamate (6 % Ni film content). In its XRD pattern, a small hcp (10.0) peak was detected at  $2\theta \sim 41^\circ$  with the hcp (11.0) main peak. When the Ni concentration was done 0.15 M (25 % Ni film content) a mixture of face centered cubic (fcc) and hcp phase formed as seen in Fig. 5. Additionally, it was suggested that the high  $H_c$  values (109 and 105 Oe) may be due to the (10.0) hcp plane detected in the XRD patterns of

the films with 6 and 25 % Ni contents. For 0.25 and 0.45 M Ni concentrations (39 and 57 at.% Ni contents, respectively), the peaks occurred from the reflections of only fcc phase were obtained. These are (111), (200), (220) and (311) peaks. Thus, it was understood that the hcp crystal structure can be changed gradually to fcc phase, when the Ni content of the films increases from 0 to 39 % or higher values. In other words, the proportion of fcc phase increases as the Ni content in the deposits increases. Strong grain boundary segregation in the investigated Ni–Co films may be responsible for the disappearance of the hcp phase at lower Co contents. It was earlier reported in our study [7] that while the film with 58 % Co content has an fcc crystal structure the film with 64 % Co content has an fcc + hcp structure. Since the film with 61 % Co content in the present study has the fcc phase, the Co content value can be determined as 62–64 % for changing of crystal structure from fcc to fcc + hcp phase.

Figure 6 shows the SEM micrographs of the films deposited from electrolytes with different Ni concentrations from 0 to 0.45 M. The surface morphology is very rough and looks like a surface of an emery paper when the Co content is significantly higher than the Ni content of the films. These morphologies are seen in the surfaces of the films containing 0 and 6 % Ni content (Fig. 6a, b). Also, the same surface appearance was observed for a film having 20 % Ni content in our earlier study [7]. The morphology becomes nearly acicular and acicular structure, when Ni content increases to 25 and 39 %, respectively, see Fig. 6c, d. Besides, it is possible to observe the clear transition from spherical granular morphology to acicular morphology, since the grains in Fig. 6c are bigger than those of Fig. 6b and thicker than those of Fig. 6d. In Fig. 6c, the surface morphology seems as a mixture of spherical granular and acicular morphologies. Thus, the film content region can be more accurately detected for transition of morphology from spherical granular to acicular morphology when the present study and the study [7] are considered. Furthermore, the all surface morphologies which were observed in the present study are compatible with the previous study [7]. In addition, it is obviously seen in the Fig. 3 that the decrease of  $M_s$  with increasing Ni content deviates from linearity. The reason for this deviation can be attributed to the grain boundary segregation of the crystallites in the Ni–Co films which have micrometer scaled grain sizes, as seen in the SEM micrographs. Straumal et al. [20] have recently demonstrated that in the case of low grain size, the grain boundary segregation of components can lead to a deviation from linear change of  $M_s$ , depending on the content of alloy.

The LMR and TMR curves of the films are given in Fig. 7. Figure 7a shows the LMR and TMR curves of the Co film and Fig. 7b represents those of the film deposited from electrolyte with 0.05 M Ni concentration

(6 % Ni film content). As seen in the figures, the TMR values are around 3.5–4 % for both of the films. However, the LMR value increases from around 3.5 to around 5 %, when the Ni content increases from 0 to 6 %. In other words, the content change of 6 % has more significant effect on LMR compared to TMR. Also, the figures reveal that as the magnetic field increases LMR increases, while TMR decreases. Therefore, it can be concluded that the detected MR type is the anisotropic magnetoresistance as found in [12, 18].

#### 4 Conclusions

In the present study, the Ni–Co films were studied by considering their crystal structures, surface morphologies, magnetic and magnetotransport properties. Since the results obtained in this study and the study [7] show similarities, it can be concluded that the properties of Ni–Co films are independent of the type of cation varying in the electrolyte consisted of nickel sulfamate and cobalt sulfate. The characteristics of Ni–Co films are mainly affected by different film contents caused by the variation of nickel sulfamate concentration in the electroplating bath. The Co and Ni codeposition occurs as the anomalous type in the 57–100 % Co concentration region which was unexplained in our earlier study [7]. The crystal structure and the surface morphology of the Ni–Co films vary depending on the Co content regions of 62–64 and 75 at.%, respectively.

**Acknowledgments** The authors are grateful to Prof. Dr. Halil Guler for XRD measurements in Balikesir University/Turkey. Also, they would like to thank Bilkent University/Turkey—UNAM, Institute of Materials Science and Nanotechnology for SEM micrographs and EDX measurements. This work was financially supported by Balikesir University under Grant no. BAP 2010/34, under Grant no. BAP 2001/02 for MR system, by Uludag University under Grant no. UAP(F)-2010/56, by The Scientific and Technological Research Council of Turkey under Grant no. TBAG-1771 for electrodeposition

system, and by State Planning Organization/Turkey under Grant no. 2005K120170 for VSM system.

#### References

1. R. Oriňáková, A. Oriňák, G. Vering, I. Talian, R.M. Smith, H.F. Arlinghaus, *Thin Solid Films* **516**, 3045–3050 (2008)
2. M. Alper, H. Kockar, H. Kuru, T. Meydan, *Sens. Actuators, A* **129**, 184–187 (2006)
3. M. Alper, H. Kockar, M. Safak, M.C. Baykul, *J. Alloys Compd.* **453**, 15–19 (2008)
4. S. Arnyanov, *Electrochim. Acta* **45**, 3323–3335 (2000)
5. L. Wang, Y. Gao, Q. Xue, H. Liu, T. Xu, *Appl. Surf. Sci.* **242**, 326–332 (2005)
6. C. Lupi, A. Dell’Era, M. Pasquali, P. Imperatori, *Surf. Coat. Technol.* **205**, 5394–5399 (2011)
7. A. Karpuz, H. Kockar, M. Alper, O. Karaagac, M. Haciismailoglu, *Appl. Surf. Sci.* **258**, 4005–4010 (2012)
8. C.K. Chung, W.T. Chang, *Thin Solid Films* **517**, 4800–4804 (2009)
9. B.G. Toth, L. Peter, A. Revesz, J. Padar, I. Bakonyi, *Eur. Phys. J. B* **75**, 167–177 (2010)
10. M. Srivastava, V.E. Selvi, V.K.W. Grips, K.S. Rajam, *Surf. Coat. Technol.* **201**, 3051–3060 (2006)
11. A. Karpuz, H. Kockar, M. Alper, *Appl. Surf. Sci.* **257**, 3632–3635 (2011)
12. H. Kockar, M. Alper, T. Sahin, M. Safak Haciismailoglu, *J. Nanosci. Nanotechnol.* **10**, 7639–7642 (2010)
13. M. Safak, M. Alper, H. Kockar, *J. Magn. Magn. Mater.* **304**, e784–e786 (2006)
14. A. Karpuz, H. Kockar, M. Alper, *Appl. Surf. Sci.* **258**, 5046–5051 (2012)
15. A. Karpuz, M. Alper, H. Kockar, *Sens. Lett.* **7**, 1–4 (2009)
16. H. Kockar, M. Alper, H. Topcu, *Eur. Phys. J. B* **42**, 497–501 (2004)
17. D. Jiles, *Introduction to magnetism and magnetic materials* (Chapman and Hall, London, 1991)
18. H. Kuru, M. Alper, H. Kockar, *J. Optoelectron. Adv. Mater–Symp.* **1**(3), 432–435 (2009)
19. D. Kim, D.-Y. Park, B.Y. Yoo, P.T.A. Sumodjo, N.V. Myung, *Electrochim. Acta* **48**, 819–830 (2003)
20. B.B. Straumal, A.A. Mazilkin, S.G. Protasova, S.V. Dobatkin, A.O. Rodin, B. Baretzky, D. Goll, G. Schütz, *Mater. Sci. Eng. A* **503**, 185–189 (2009)